Date of publication JUN-30, 2025, date of current version MAY-08, 2025.
www.computingonline.net / computing@computingonline.net

Print ISSN 1727-6209
Online ISSN 2312-5381
DOI 10.47839/ijc.24.2.4006

Long-term Land Surface Temperature Forecasting in Different Climate Zones using Long Short-term Memory

TETIANA HOVORUSHCHENKO[1], OLGA PAVLOVA[1], VITALII ALEKSEIKO[1], ANDRII KUZMIN[1], ELENA ZAITSEVA[2]
[1]Computer Engineering and Information Systems Department, Khmelnytskyi National University, 29016, Khmelnytskyi, Ukraine
[2]Department of Informatics, Zilina University, Univerzitná 8215, 010 26 Žilina, Slovakia

Corresponding author: Vitalii Alekseiko (e-mail: vitalii.alekseiko@khmnu.edu.ua).

ABSTRACT Climate change, which has been observed for several decades, is becoming increasingly widespread. The consequences of such changes are a negative impact on ecosystems in different regions of the planet, as well as on the biosphere. The Sustainable Development Goals define climate action as one of the key goals, which covers a wide range of actions to avoid and mitigate the consequences caused by climate change. To preserve biodiversity, increase the safety of residents of cities and communities located in vulnerable regions, it is necessary to form an integrated approach that will ensure sustainable development and improve the quality of life. Understanding the future climate situation and potential consequences is impossible without high-quality forecasting of climate indicators. One of the main indicators is the temperature of the Earth's surface. The article analyzes the use of a recurrent neural network with a long short-term memory for long-term forecasting of temperature in different climatic zones. A study of the forecast accuracy for different time periods, considering climatic zoning, was conducted. The results indicate the feasibility of using the proposed approach for forecasting future Earth surface temperatures based on historical data.

KEYWORDS recurrent neural networks; long short-term memory; long-term temperature forecasting; temperature regime; climatic zones; land surface temperature.

I. INTRODUCTION

Forecasting number series is an important task in the field of climate monitoring. Analysis of changes in climatic indicators such as temperature, precipitation, sea level, etc., allows for comprehensive monitoring of changes and prediction of negative consequences.

The World Meteorological Organization (WMO) has officially confirmed that 2024 was the warmest year on record. The previous warmest year, by a significant margin, was 2023 [1]. This indicates an annual trend of increasing temperatures.

One of the important aspects of climate change research is the study of changes in Land Surface Temperature (LST). The temperature of the Earth's surface is affected by a number of factors, in particular:

- solar radiation;
- movement of air masses;
- geographical latitude;
- height above sea level;
- distance to large bodies of water;
- type of relief;
- type of soil.

Thus, the LST is influenced by a combination of factors, and for accurate forecasting it is necessary to conduct a comprehensive analysis of a specific region, which is extremely costly in terms of resources involved. On the other hand, the study of historical data [2] and their main trends can significantly simplify the forecasting task.

II. DOMAIN ANALYSIS

Previous works analyzed the application of machine learning methods for forecasting LST in the short- and medium-term [3], investigated its role in the context of the development of sustainable cities and communities [4], proposed the concept of an information system, and identified the features of its design [5].

Various technologies and approaches are used to forecast time series. It is used different techniques for time-series analysis [6-8].

The article [9] discusses the long-term time series forecasting model SparseTSF, which is based on the Cross-Period Sparse Forecasting technique, which simplifies the forecasting task by separating periodicity and trends in time series data.

The study [10] examines the use of deep learning techniques and presents a hybrid model that combines convolutional neural networks (CNN) and long short-term memory (LSTM) networks to predict historical temperature data.

In the research [11] presented LSTM model which uses Global Temperature Data for climate forecasting.

In the article [12] presented a predictive model for predicting future values of multivariate temperature Time Series.

The research [13] presents data-driven approaches for LST forecasting in Tiruchirappalli, India.

The study [14] analyzes the use of machine learning methods XG-Boost, Bagging-XG-Boost, and AdaBoost for forecasting satellite data obtained using Landsat-8.

Series with seasonal patterns are predicted with high accuracy for short-term forecasting by autoregressive ARIMA models [15] and their modifications [16-18], as well as by classical machine learning methods (random forest, gradient boosting) [19, 20]. However, for long-term forecasting, it is advisable to consider more complex models, in particular recurrent neural networks (RNNs) [21-23], including the LSTM [24, 25] method or combination of RNN with CNNs [26-32] or other technologies (e.g. Transformer-Based models [33, 34], modified RNN [35]).

Based on the analysis, it is advisable to conduct a study of the effectiveness of using LSTM for forecasting LST. It is planned to conduct research for each climatic zone and each hemisphere. The exceptions are countries and regions located simultaneously in both hemispheres, since there are complex patterns that are difficult to predict, as well as the lack of results for the continental type of climate in the southern hemisphere, due to its absence, due to the lack of continental territories sufficient for the formation of this type of climate [36].

III. METHODOLOGY

Methodology of the research presented in Figure 1.

A. DATASET STRUCTURE

It should be noted that it is impossible to accurately establish dependencies based on short-term observations, therefore, the analysis of climate data requires accurate measurements, long-term observations and modern data processing methods. This is a complex and multifaceted task, the solution of which will contribute to the development of effective strategies for adapting to climate change and reducing its negative consequences. Therefore, data covering a significant period of time should be selected for training the model. It is used the GlobalLandTemperatures dataset [37] from the Kaggle platform. The dataset was modified due to the specifics of the study by establishing correspondences between countries and the climatic zones in which they are located [38].

B. LONG SHORT-TERM MEMORY

An LSTM model is a type of RNN that is suitable for time series forecasting due to its ability to store information for both short and long periods of time [39, 40].

The LSTM architecture involves three main gates (forget, input, and output) that control the flow of information [41].

The forget gate decides which information from the previous state of the cell should be discarded. In formalized form, the function has the form:

$$f_t = \sigma(W_f \cdot [h_{t-1}, x_t] + b_f), \tag{1}$$

where f_t – activation function of the forgetting gate, x_t – input parameter of time t, h_{t-1} – hidden state from the previous time step, W_f – weight matrix, b_f – bias, σ – sigmoid activation function.

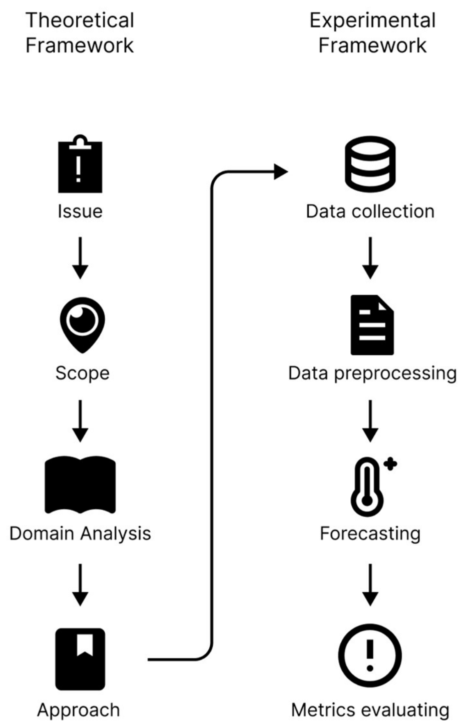

Figure 1. Research Methodology.

The input gate determines what new information will be stored in the cell state. It consists of two parts:

$$i_t = \sigma(W_i \cdot [h_{t-1}, x_t] + b_i), \tag{2}$$

where i_t – activation of the entrance gate.

$$\tilde{C}_t = tanh(W_C \cdot [h_{t-1}, x_t] + b_C), \tag{3}$$

where $\tilde{C}_t$ – candidate cell state.

The state of the cell C_t at time t is updated using the forget gate and the input gate:

$$C_t = f_t \cdot C_{t-1} + i_t \cdot \tilde{C}_t, \tag{4}$$

The output gate controls the output of the cell state by affecting the hidden state h_t:

$$o_t = \sigma(W_o \cdot [h_{t-1}, x_t] + b_o), \tag{5}$$
$$h_t = o_t \cdot \tanh(C_t). \tag{6}$$

These gates allow the LSTM to retain relevant past information, discarding what is not needed, solving the problem of gradient vanishing that is commonly encountered in RNNs, and allowing the LSTM to capture long-term dependencies.

In the context of LST forecasting, short-term dependencies are necessary to capture instantaneous weather variations, while long-term dependencies allow the model to recognize seasonal trends, cycles, and anomalies over longer periods of time.

The state of the C_t cell helps maintain an internal representation of LST patterns over long periods, which is particularly useful for recognizing patterns such as annual temperature cycles, temperature anomalies, and gradual climate trends.

During training, LSTMs use backpropagation in time (BPTT) to optimize the weights associated with each gate. The objective function that is commonly used is the mean square error (MSE):

$$MSE = \frac{1}{n}\sum_{i=1}^{n}(y_i - \hat{y}_i)^2, \quad (7)$$

where n – the number of observations, y_i – the actual value of the i-th observation, $\hat{y}_i$ – is the predicted value of the i-th observation.

Figure 2 displays LSTM memory cell.

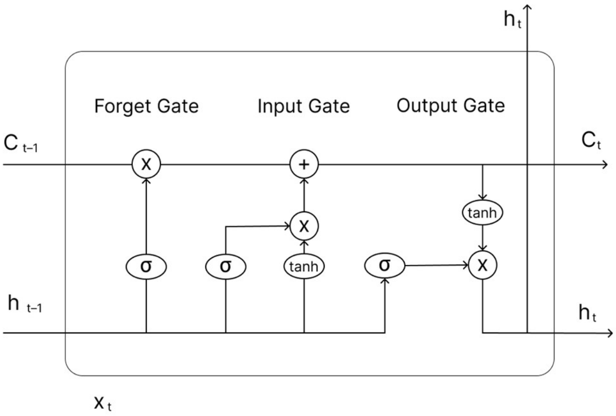

Figure 2. LSTM memory cell.

IV. CASE STUDY & RESULTS

Typically, machine learning model evaluation is performed by splitting the initial sample in a ratio of 1 to 4, where the training set is the largest part, however, given the lack of a sufficient number of measurements, the approach is slightly modified in this study. The model was fitted on data from 1800 to 1900 and then tested in each climate zone to make a 100-year forecast (1900-2000). Although current climate trends are changing rapidly, it should be noted that the study period covers the times of the Industrial Revolution, meaning that the climate indicators of this period cannot be considered stable.

The study was conducted for a model with LSTM architecture, 50 epochs were used for training. Adam was chosen as the optimizer. The loss function was estimated using the mean square error.

Figure 3 and 4 show training and validation loss for tropical climate zone.

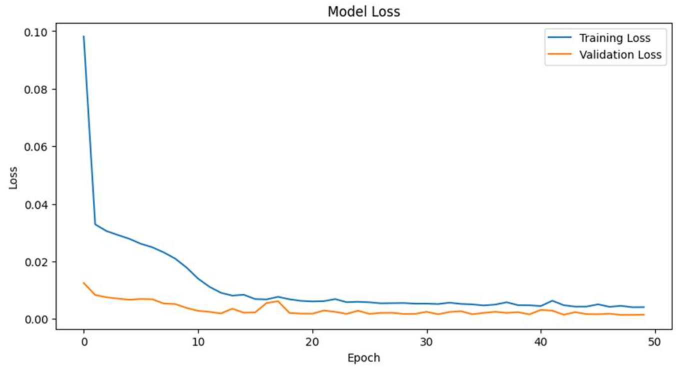

Figure 3. Training and validation loss for tropical climate zone in North Hemisphere.

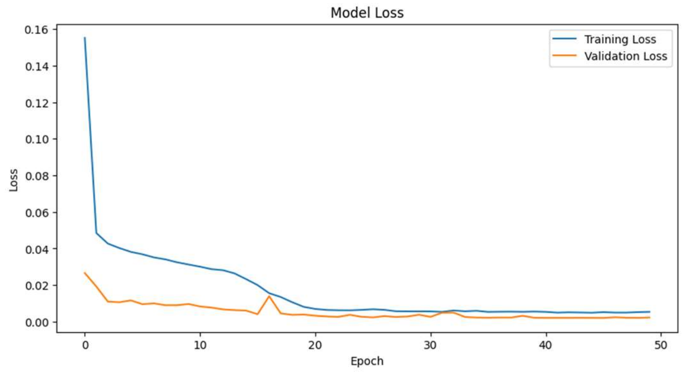

Figure 4. Training and validation loss for tropical climate zone in South Hemisphere.

Figures 5 and 6 show forecasted and observed temperatures in tropical climate zone in North Hemisphere and Figures 7 and 8 in South Hemisphere for first and last decades of 20th century.

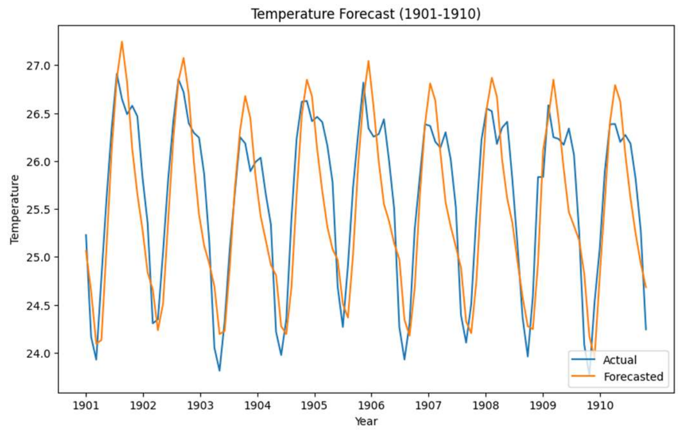

Figure 5. Forecasted and observed temperatures in tropical climate zone in North Hemisphere in first decade of 20th century.

The graphs clearly show that the model tries to smooth the data at the top of the curve. The maximum temperatures for the studied region have a somewhat unusual character compared to other climate zones, which will be discussed below. First, there is a maximum of annual temperatures, after which there is a slight decrease in temperature, and then an increase again before a monotonous decline to a minimum.

However, such a sequence is not observed every year, which makes the tropical climate zone a difficult region to predict. Based on this, forecasting in the region using the LSTM method is inefficient, therefore it is advisable to conduct additional analysis of the considered Time Series.

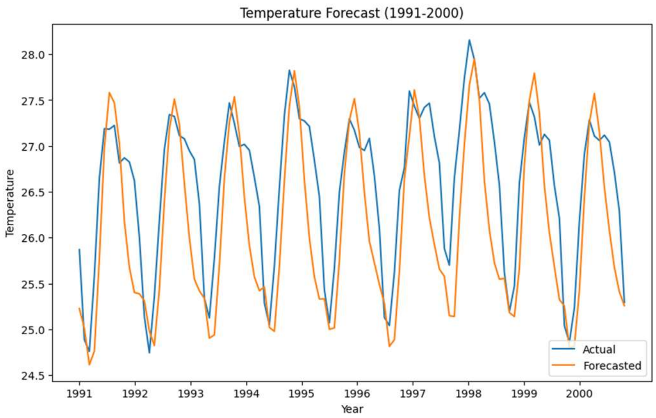

Figure 6. Forecasted and observed temperatures in tropical climate zone in North Hemisphere in last decade of 20th century.

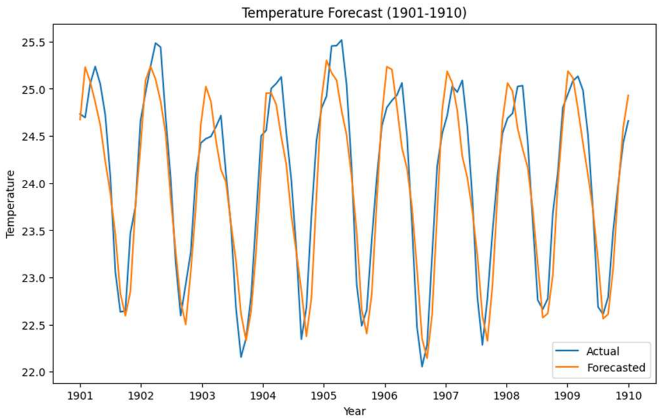

Figure 7. Forecasted and observed temperatures in tropical climate zone in South Hemisphere in first decade of 20th century.

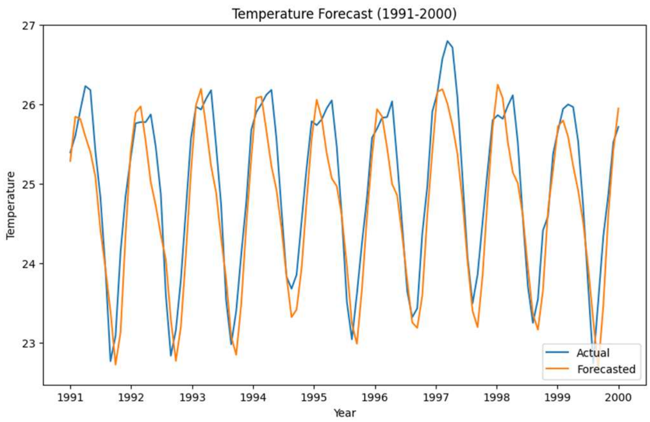

Figure 8. Forecasted and observed temperatures in tropical climate zone in South Hemisphere in last decade of 20th century.

Table 1 presents the calculated metrics for each decade of the 20th century for the tropical climate zone.

The values of the metrics indicate the impossibility of using the model for forecasting. The R^2 metric demonstrates a downward trend in the Northern Hemisphere, which indicates the inability of the model to capture changes. At the same time, in the Southern Hemisphere, the metric indicators, although remaining low, demonstrate some stability.

Table 1. Metrics evaluation for tropical climate zone.

Decade	MAE	MSE	RMSE	R^2 Score
North Hemisphere				
1901–1910	0.4085	0.2190	0.4680	0.7176
1911–1920	0.4048	0.2250	0.4743	0.6931
1921–1930	0.4371	0.2610	0.5109	0.6041
1931–1940	0.4172	0.2453	0.4953	0.6060
1941–1950	0.4474	0.2849	0.5337	0.5392
1951–1960	0.5240	0.3780	0.6148	0.4532
1961–1970	0.4709	0.3323	0.5764	0.5058
1971–1980	0.5025	0.3667	0.6055	0.4913
1981–1990	0.5363	0.4163	0.6452	0.3960
1991–2000	0.5586	0.4729	0.6877	0.3296
South Hemisphere				
1901–1910	0.3149	0.1404	0.3748	0.8483
1911–1920	0.3440	0.1709	0.4135	0.8446
1921–1930	0.3612	0.1884	0.4340	0.8446
1931–1940	0.3536	0.1741	0.4172	0.8355
1941–1950	0.3609	0.1804	0.4247	0.8358
1951–1960	0.3792	0.2009	0.4482	0.8216
1961–1970	0.3546	0.1820	0.4266	0.8366
1971–1980	0.3848	0.1976	0.4446	0.8101
1981–1990	0.4028	0.2254	0.4747	0.8027
1991–2000	0.3988	0.2322	0.4819	0.7883

Figures 9 and 10 demonstrate training and validation loss for dry or arid climate zone.

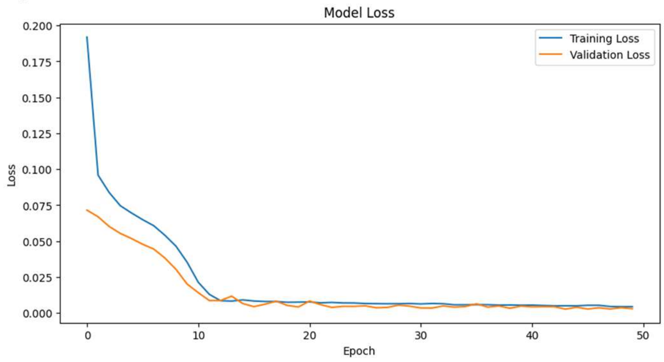

Figure 9. Training and validation loss for arid climate zone in North Hemisphere.

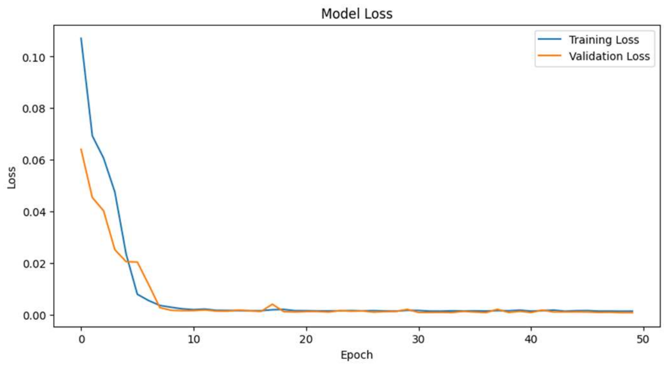

Figure 10. Training and validation loss for arid climate zone in South Hemisphere.

Figures 11 and 12 show forecasted and observed temperatures in arid climate zone in North Hemisphere and Figures 13 and 14 in South Hemisphere for first and last decades of 20th century. In this climate zone, high accuracy is observed for the Northern Hemisphere, since the graphs almost coincide.

Vice versa in the Southern Hemisphere, model doesn't follow increasing trend.

Table 2 highlights metrics evaluation for arid climate zone.

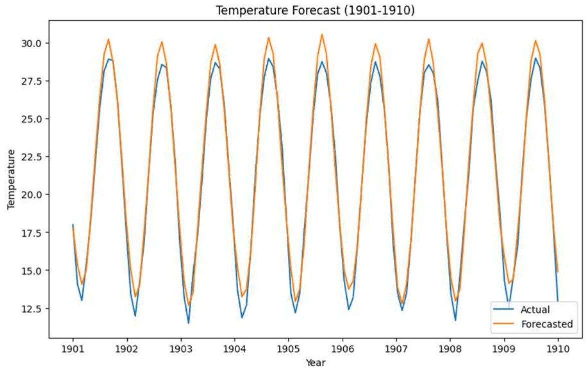

Figure 11. Forecasted and observed temperatures in arid climate zone in North Hemisphere in first decade of 20th century.

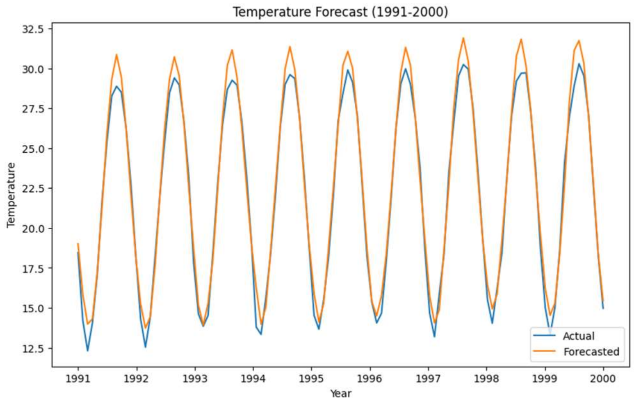

Figure 12. Forecasted and observed temperatures in arid climate zone in North Hemisphere in last decade of 20th century.

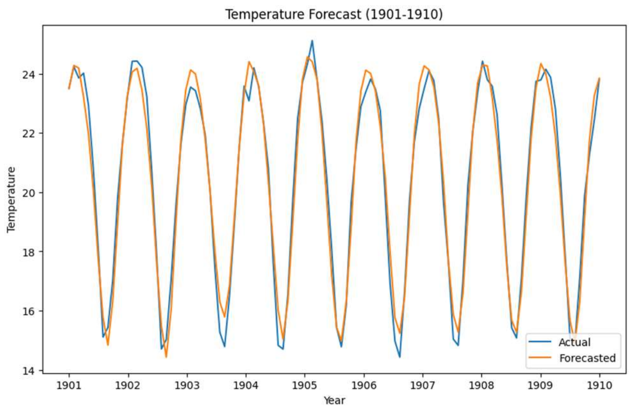

Figure 13. Forecasted and observed temperatures in arid climate zone in South Hemisphere in first decade of 20th century.

For the dry climate zone, there is a significant difference between the forecast results in the Northern and Southern Hemispheres. In the Northern Hemisphere, the forecast demonstrates high accuracy throughout the century. Thus, the model captures patterns well and allows long-term forecasting of the LST values with high accuracy. At the same time, for the Southern Hemisphere, there is a decrease in forecast accuracy over time, i.e. the model is suitable for short-term forecasting, but does not capture long-term trends.

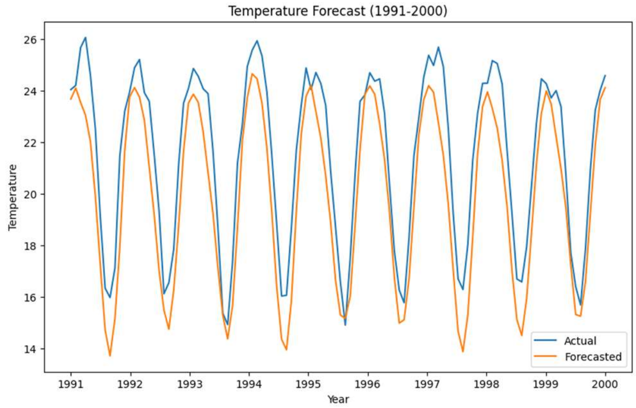

Figure 14. Forecasted and observed temperatures in arid climate zone in South Hemisphere in last decade of 20th century.

Table 2. Metrics evaluation for arid climate zone.

Decade	MAE	MSE	RMSE	R^2 Score
North Hemisphere				
1901–1910	0.7043	0.6873	0.8291	0.9800
1911–1920	0.6839	0.7127	0.8442	0.9785
1921–1930	0.7832	0.8985	0.9479	0.9735
1931–1940	0.7667	0.8362	0.9144	0.9747
1941–1950	0.7968	0.8979	0.9476	0.9735
1951–1960	0.7042	0.7124	0.8440	0.9780
1961–1970	0.7146	0.8032	0.8962	0.9749
1971–1980	0.8094	0.9483	0.9738	0.9718
1981–1990	0.7718	0.8190	0.9050	0.9761
1991–2000	0.7004	0.7355	0.8576	0.9784
South Hemisphere				
1901–1910	0.5438	0.4299	0.6556	0.9608
1911–1920	0.8328	0.9463	0.9728	0.9225
1921–1930	0.8756	1.0667	1.0328	0.9163
1931–1940	0.8464	1.0011	1.0005	0.9151
1941–1950	1.0586	1.5293	1.2367	0.8725
1951–1960	0.9620	1.3136	1.1462	0.8885
1961–1970	1.0932	1.5764	1.2555	0.8712
1971–1980	0.9836	1.4951	1.2227	0.8714
1981–1990	1.6086	3.1377	1.7714	0.7283
1991–2000	1.7892	3.9845	1.9961	0.6383

Figures 15 and 16 demonstrate training and validation loss for temperate climate zone.

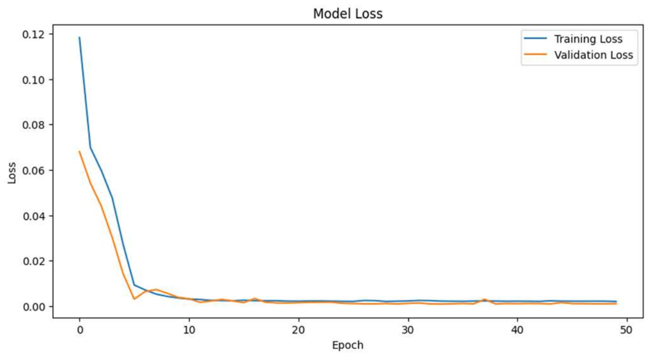

Figure 15. Training and validation loss for temperate climate zone in North Hemisphere.

Figures 17 and 18 show forecasted and observed temperatures in arid climate zone in North Hemisphere and Figures 19 and 20 in South Hemisphere for first and last decades of 20th century. The graph indicates that in the temperate climate zone, different amplitudes of oscillations are observed, that is, the minimum and maximum values vary unevenly each year within certain ranges. Models are difficult to capture this pattern, although data that are not extremes are predicted with high accuracy.

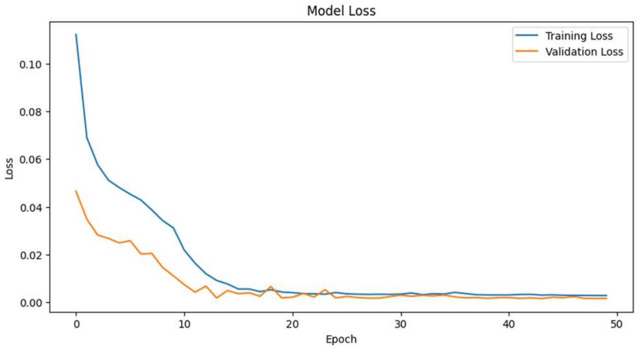

Figure 16. Training and validation loss for temperate climate zone in South Hemisphere.

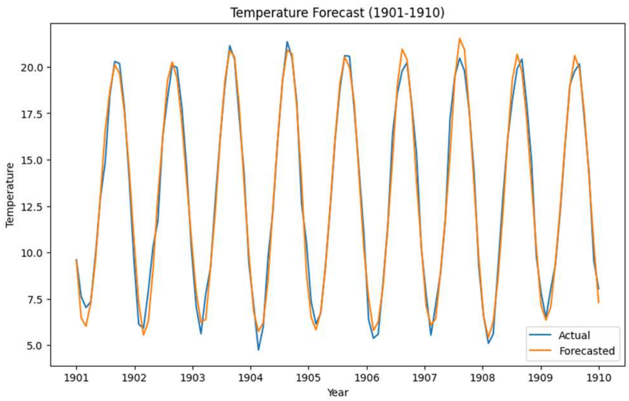

Figure 17. Forecasted and observed temperatures in temperate climate zone in North Hemisphere in first decade of 20th century.

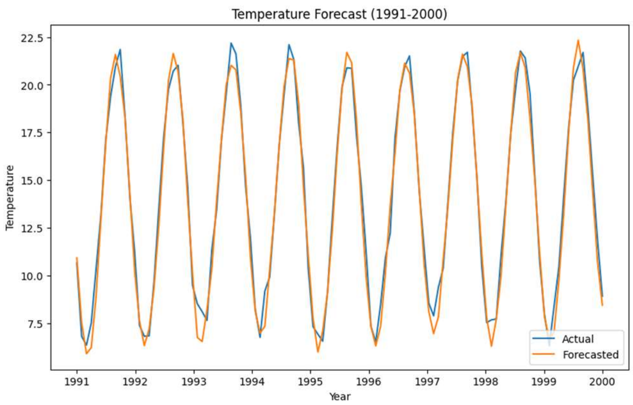

Figure 18. Forecasted and observed temperatures in temperate climate zone in North Hemisphere in last decade of 20th century.

Table 3 shows metrics evaluation for temperate climate zone. For the temperate climate zone, a similar trend is observed in both hemispheres. In the Northern Hemisphere, the indicators are somewhat higher. The values of the R2 metric indicate the possibility of using the model for long-term forecasting. At the same time, for the Southern Hemisphere, the values remain quite high, but are insufficient, so the model needs to be refined and improved.

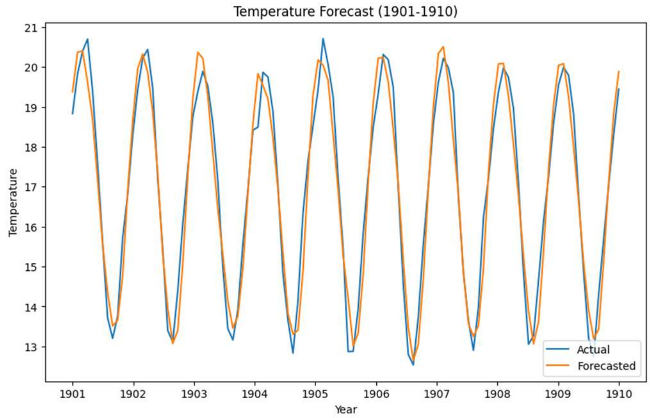

Figure 19. Forecasted and observed temperatures in temperate climate zone in South Hemisphere in first decade of 20th century.

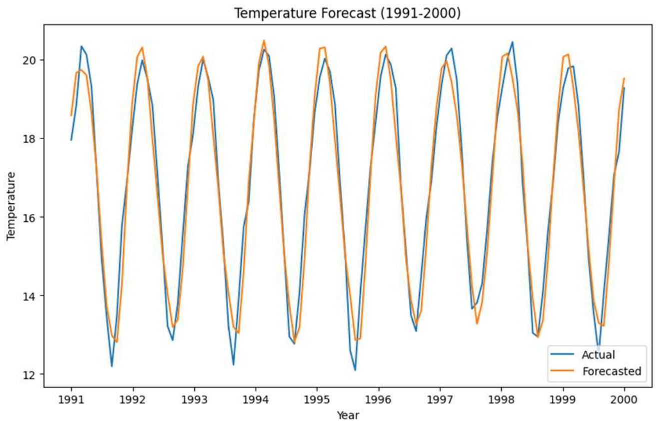

Figure 20. Forecasted and observed temperatures in temperate climate zone in South Hemisphere in last decade of 20th century.

Table 3. Metrics evaluation for temperate climate zone.

Decade	MAE	MSE	RMSE	R^2 Score
North Hemisphere				
1901–1910	0.6685	0.6524	0.8077	0.9757
1911–1920	0.7095	0.7723	0.8788	0.9686
1921–1930	0.6840	0.7572	0.8702	0.9717
1931–1940	0.6956	0.7653	0.8748	0.9722
1941–1950	0.7084	0.7544	0.8686	0.9739
1951–1960	0.6166	0.6709	0.8191	0.9748
1961–1970	0.7380	0.7998	0.8943	0.9710
1971–1980	0.6096	0.5331	0.7301	0.9784
1981–1990	0.6428	0.6540	0.8087	0.9760
1991–2000	0.6431	0.5886	0.7672	0.9781
South Hemisphere				
1901–1910	0.5438	0.3995	0.6321	0.9366
1911–1920	0.5369	0.4110	0.6411	0.9393
1921–1930	0.5245	0.3756	0.6129	0.9484
1931–1940	0.5019	0.3744	0.6119	0.9432
1941–1950	0.5774	0.4841	0.6958	0.9343
1951–1960	0.5035	0.3812	0.6174	0.9432
1961–1970	0.5107	0.3791	0.6157	0.9427
1971–1980	0.4915	0.3686	0.6071	0.9427
1981–1990	0.4554	0.2967	0.5447	0.9549
1991–2000	0.5458	0.4205	0.6484	0.9337

Figure 21 demonstrates training and validation loss for temperate climate zone.

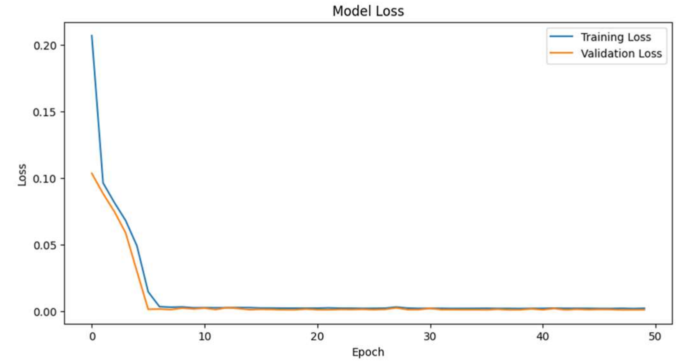

Figure 21. Training and validation loss for continental climate zone.

Figures 22 and 23 show forecasted and observed temperatures in continental climate zone.

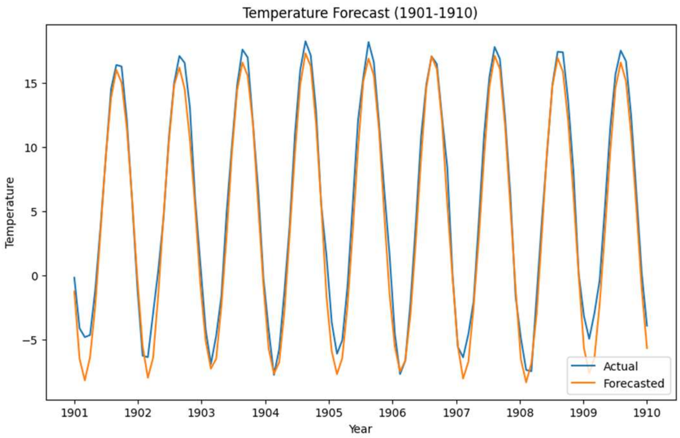

Figure 22. Forecasted and observed temperatures in continental climate zone in first decade of 20th century.

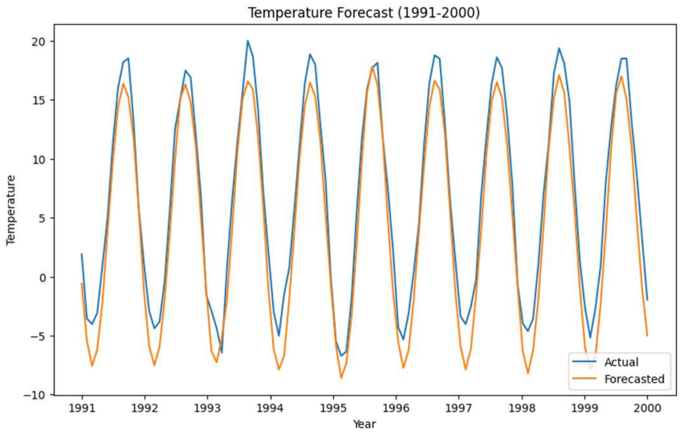

Figure 23. Forecasted and observed temperatures in continental climate zone in last decade of 20th century.

Table 4 presents metrics evaluation for continental climate zone.

Metrics for the continental climate zone are high, meaning the model is suitable for predicting data for this type of climate. Slightly higher error rates are observed than for the tropical, arid, and temperate climate zones, which is due to the larger temperature amplitude characteristic of this type of climate.

Table 4. Metrics evaluation for continental climate zone.

Decade	MAE	MSE	RMSE	R^2 Score
North Hemisphere				
1901–1910	0.7468	0.9031	0.9503	0.9876
1911–1920	0.8898	1.2080	1.0991	0.9834
1921–1930	0.9705	1.5181	1.2321	0.9804
1931–1940	1.1403	1.8850	1.3729	0.9760
1941–1950	1.0967	1.7626	1.3276	0.9779
1951–1960	0.9940	1.5310	1.2374	0.9796
1961–1970	1.0048	1.5381	1.2402	0.9805
1971–1980	0.9077	1.3784	1.1740	0.9808
1981–1990	1.2662	2.3105	1.5200	0.9689
1991–2000	1.3862	2.6174	1.6178	0.9632

Figures 24 and 25 demonstrate training and validation loss for polar climate zone.

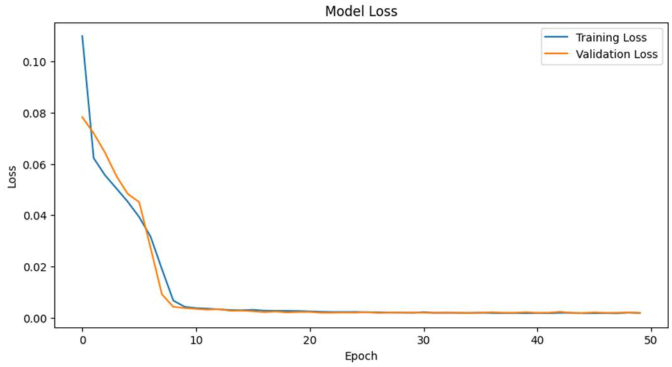

Figure 24. Training and validation loss for polar climate zone in North Hemisphere.

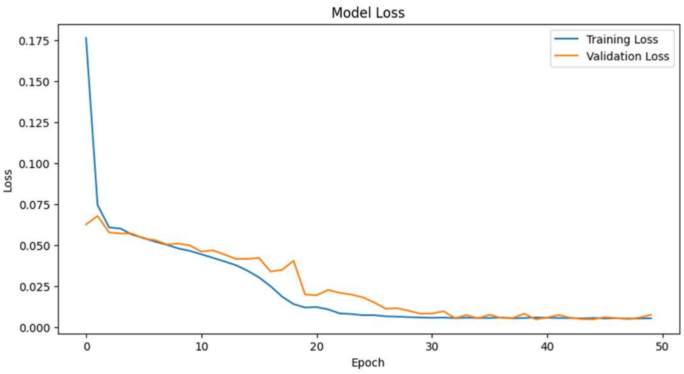

Figure 25. Training and validation loss for polar climate zone in South Hemisphere.

Figures 26 and 27 show forecasted and observed temperatures in arid climate zone in North Hemisphere and Figures 28 and 29 in South Hemisphere for first and last decades of 20th century. Similar to the tropical climate zone, maximum and minimum temperature data in the polar climate zone can vary. Although the graphs show that the model is trying to adapt to the characteristics of this climatic zone, demonstrating a forecast without smoothing the extremes, the pattern of the forecast values does not always correspond to the pattern that is actually observed.

Table 5 demonstrates metrics evaluation for polar climate zone.

The R^2 metric indicators, close to 95%, indicate sufficient forecasting accuracy for using the proposed model in the polar climatic zone of the Northern Hemisphere, however, significantly lower indicators are observed in the Southern

Hemisphere, which indicates the need to improve the model in order to enable accurate forecasting in the fire region of the Southern Hemisphere.

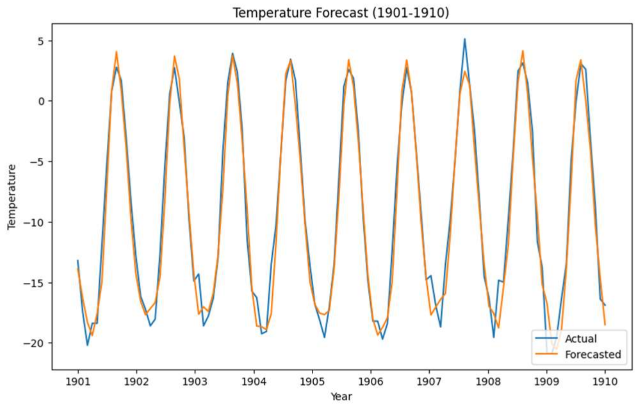

Figure 26. Forecasted and observed temperatures in polar climate zone in North Hemisphere in first decade of 20th century.

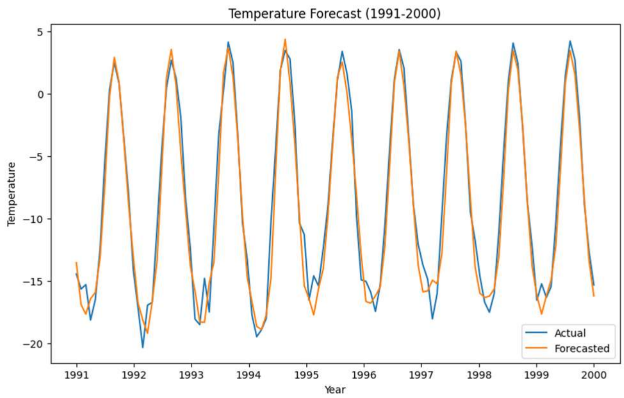

Figure 27. Forecasted and observed temperatures in polar climate zone in North Hemisphere in last decade of 20th century.

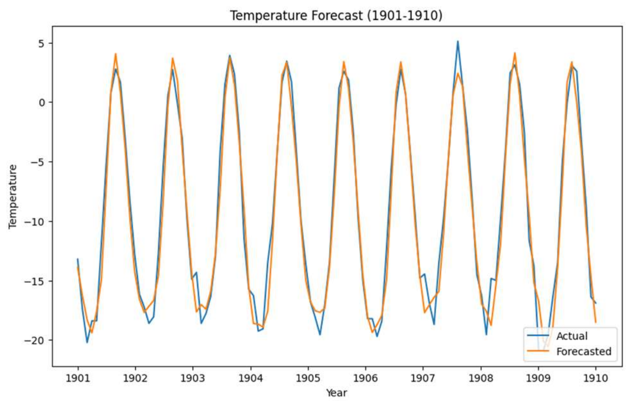

Figure 28. Forecasted and observed temperatures in polar climate zone in South Hemisphere in first decade of 20th century.

Long-term LST forecasting plays a key role in achieving the Sustainable Development Goals (SDGs) by enabling informed decision-making on environmental sustainability, climate change resilience and human well-being.

Long-term LST forecasting helps to predict future climate parameters and, as a result, identify potential periods of extreme temperature fluctuations, heat waves, droughts and other impacts of climate change.

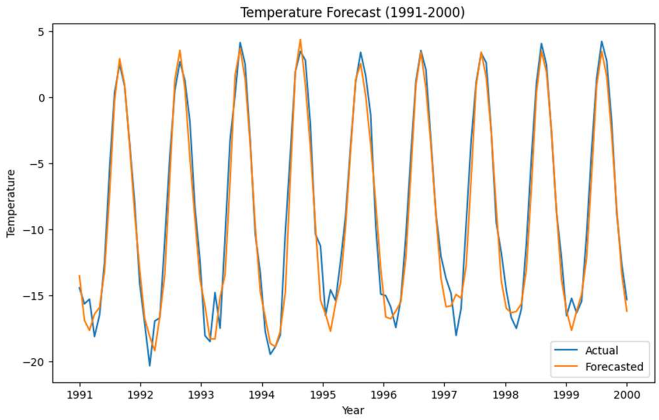

Figure 29. Forecasted and observed temperatures in polar climate zone in South Hemisphere in last decade of 20th century.

Table 5. Metrics evaluation for polar climate zone.

Decade	MAE	MSE	RMSE	R^2 Score
North Hemisphere				
1901–1910	1.1667	2.1028	1.4501	0.9669
1911–1920	1.2794	2.8402	1.6853	0.9544
1921–1930	1.1427	2.0580	1.4346	0.9610
1931–1940	1.2723	2.8613	1.6916	0.9477
1941–1950	1.0931	2.1041	1.4506	0.9615
1951–1960	0.9606	1.4867	1.2193	0.9728
1961–1970	1.0962	2.0643	1.4368	0.9622
1971–1980	1.2866	2.9787	1.7259	0.9473
1981–1990	1.0849	1.9899	1.4107	0.9665
1991–2000	1.1057	1.9444	1.3944	0.9663
South Hemisphere				
1901–1910	0.8300	1.0868	1.0425	0.8306
1911–1920	0.8904	1.2883	1.1350	0.8127
1921–1930	0.8654	1.2769	1.1300	0.7955
1931–1940	0.9181	1.3060	1.1428	0.7816
1941–1950	0.8448	1.2414	1.1142	0.7812
1951–1960	0.9131	1.2384	1.1128	0.7864
1961–1970	0.8019	0.9435	0.9713	0.8099
1971–1980	0.8636	1.1667	1.0801	0.8123
1981–1990	0.8903	1.2544	1.1200	0.7918
1991–2000	0.7117	0.8503	0.9221	0.8496

Thus, accurate forecasting will contribute to increasing the preparedness of communities to extreme climate events, including extreme heat or cold, droughts, forest fires, etc.

V. DISCUSSION

The conducted study allows us to conclude that the use of a neural network with LSTM architecture for predicting the temperature regime of the earth's surface demonstrates different accuracy in different climatic zones. Thus, the use of the proposed model is highly effective for predicting clearly expressed seasonal dependencies observed in arid, temperate and continental climatic zones. At the same time, the equatorial climatic zone has distinctive patterns that are not always captured.

Another important aspect is the limitation of the proposed approach due to the lack of accurate instruments and technologies for measuring the temperature of the earth's surface over significant time periods in certain regions. Such inaccuracies can provoke errors in the data and affect the forecasting. At the same time, the emergence of modern technologies, in particular satellite data, allows for monitoring temperatures in different regions without significant differences. However, the period of such observations is not long-term and at this stage does not allow for high-quality long-term forecasting.

Another limitation is the small amount of observational data in polar regions, which is explained by their remoteness and harsh climate. Overall, the LSTM method demonstrates high accuracy, making it suitable for predicting temperature dependences in most regions.

Analysis of LST change presents a holistic picture for government officials, indicating the effectiveness of existing strategies.

Long-term LST forecasting is key for agricultural planning, as it helps to determine the correlation between LST values and yields, predicting future crop cycles and thus improving food security.

In general, long-term LST forecasting can help achieve some SDGs as Zero Hunger (SDG-2), Good Health and Well-being (SDG-3), Sustainable Cities and Communities (SDG-11), Climate Change (SDG-13), Life on Land (SDG-15). Also there are indirect impact on some else SDGs as Life below Water (SDG-14) and Partnership for the Goals (SDG-17).

VI. CONCLUSIONS

LSTM is an effective method used for a wide range of forecasting problems. Since climate data, such as temperature indicators, represent time series, this method is appropriate to use for forecasting future climate parameters. The LSTM method is appropriate to use for the problem of long-term forecasting, given that due to its architecture, it is less prone to decay, compared to other machine learning methods, such as random forest, gradient boosting, vector regression, etc., and is also able to take into account long-term trends.

The results of experiments show different accuracy due to climate zones and hemispheres. Although in some regions model demonstrates high accuracy, but metrics in most regions are not high enough for forecasting.

There is also a significant difference in the data of the northern and southern hemispheres, which is due to geographical features. The assessment by the P2 metric shows that the proposed approach is advisable to use for forecasting in regions with clearly defined seasonality. Thus, in arid, temperate and continental zones, the results reach 95-98% in the northern and 92-95% in the southern hemispheres. Slightly lower results are observed for polar regions: 93-96% for the Arctic region and 78-85% for the Antarctic. For the tropical climatic zone, the results are not satisfactory, since they are within 70% for the northern and 80% for the southern hemisphere and demonstrate a tendency to attenuation. Thus, for the tropical region, more comprehensive studies and evaluation of various models for forecasting are required.

Thus, it is considered to provide further research to improve models' accuracy for this regions by providing data preprocessing or architecture specification.

References

[1] World Meteorological Organization. Available online: https://wmo.int/ (accessed on 21 February 2025).

[2] M. Perera, J. De Hoog, K. Bandara, D. Senanayake, & S. Halgamuge, "Day-ahead regional solar power forecasting with hierarchical temporal convolutional neural networks using historical power generation and weather data," *Applied Energy*, vol. 361, 122971, 2024. https://doi.org/10.1016/j.apenergy.2024.122971.

[3] T. Hovorushchenko, V. Alekseiko, & V. Levashenko, "Machine learning methods' comparison for land surface temperatures forecasting due to climate classification," *Proceedings of the 1st International Workshop on Advanced Applied Information Technologies AdvAIT 2024 with CEUR-WS*, Khmelnytskyi, Ukraine, Zilina, Slovakia, December 5, 2024, vol. 3899, pp. 55-68. https://ceur-ws.org/Vol-3899/paper7.pdf.

[4] T. Hovorushchenko, & V. Alekseiko, "Land surface temperature forecasting in the context of the development of sustainable cities and communities," *Computer Systems and Information Technologies*, vol. 3, pp. 6–12, 2024. https://doi.org/10.31891/csit-2024-3-1.

[5] V. Alekseiko, "Web-based information system for land surface temperature forecasting using machine learning methods," *Science and technology today*, vol. 10, issue 38, pp. 17–27, 2024. https://doi.org/10.52058/2786-6025-2024-10(38)-17-27.

[6] V. Ivanenko, V. Alekseiko, O. Klymenko, "Machine forecast evaluation: an algorithm for trends, financial indicators, and business process optimization," *Science and Technology Today*, vol. 8, issue 36, pp. 1018–1033, 2024. https://doi.org/10.52058/2786-6025-2024-8(36)-1018-1033.

[7] K. Zhang et al., "Self-supervised learning for time series analysis: Taxonomy, progress, and prospects," *IEEE Transactions on Pattern Analysis and Machine Intelligence*, vol. 46, no. 10, pp. 6775-6794, 2024. https://doi.org/10.1109/TPAMI.2024.3387317.

[8] O. Duda, et al., "Data processing in IoT for smart city systems," *Proceedings of the 2019 10th IEEE International Conference on Intelligent Data Acquisition and Advanced Computing Systems: Technology and Applications (IDAACS)*, Metz, France, 2019, pp. 96-99. https://doi.org/10.1109/IDAACS.2019.8924262.

[9] S. Lin, W. Lin, W. Wu, H. Chen, & J. Yang, "SparseTSF: Modeling long-term time series forecasting with 1k parameters," *arXiv* (Cornell University), 2024. https://doi.org/10.48550/arxiv.2405.00946.

[10] Y. Gong, Y. Zhang, F. Wang, & C. Lee, "Deep learning for weather forecasting: A CNN-LSTM hybrid model for predicting historical temperature data," *arXiv* (Cornell University), 2024. https://doi.org/10.48550/arxiv.2410.14963.

[11] P. Akhila, R. L. S. Anjana and M. Kavitha, "Climate forecasting: Long short term memory model using global temperature data," *Proceedings of the 2022 6th International Conference on Computing Methodologies and Communication (ICCMC)*, Erode, India, 2022, pp. 469-473. https://doi.org/10.1109/ICCMC53470.2022.9753779.

[12] K. Zhou, C. Zhang, B. Xu, J. Huang, C. Li, & Y. Pei, "TE-LSTM: a prediction model for temperature based on multivariate time series data," *Remote Sensing*, vol. 16, issue 19, 3666, 2024. https://doi.org/10.3390/rs16193666.

[13] A. Badugu, K. S. Arunab, & A. Mathew, "Predicting land surface temperature using data-driven approaches for urban heat island studies: a comparative analysis of correlation with environmental parameters," *Modeling Earth Systems and Environment*, vol. 10, issue 1, pp. 1043–1076, 2023. https://doi.org/10.1007/s40808-023-01822-2.

[14] C. B. Pande, J. C. Egbueri, R. Costache, L. M. Sidek, Q. Wang, F. Alshehri, N. M. Din, V. K. Gautam, & S. C. Pal, "Predictive modeling of land surface temperature (LST) based on Landsat-8 satellite data and machine learning models for sustainable development," *Journal of Cleaner Production*, vol. 444, 141035, 2024. https://doi.org/10.1016/j.jclepro.2024.141035.

[15] S. Jafarian-Namin, D. Shishebori, and A. Goli, "Analyzing and predicting the monthly temperature of Tehran using ARIMA model, artificial neural network, and its improved variant," *Journal of Applied Research on Industrial Engineering*, vol. 11, issue 1, pp. 76-92, 2024. ttps://doi.org/10.22105/jarie.2023.356297.1502.

[16] X. Chen, Z. Jiang, H. Cheng, et al., "A novel global average temperature prediction model based on GM-ARIMA combination model," *Earth Sci Inform*, vol. 17, pp. 853–866, 2024. https://doi.org/10.1007/s12145-023-01179-1.

[17] M. Elseidi, "A hybrid Facebook Prophet-ARIMA framework for forecasting high-frequency temperature data," *Model. Earth Syst. Environ.*, vol. 10, pp. 1855–1867, pp. 2024. https://doi.org/10.1007/s40808-023-01874-4.

[18] Wang, G., Su, H., Mo, L., Yi, X., & Wu, P. (2024). Forecasting of soil respiration time series via clustered ARIMA. *Computers and Electronics in Agriculture*, 225, 109315. https://doi.org/10.1016/j.compag.2024.109315.

[19] R. R. Guerra, A. Vizziello, P. Savazzi, E. Goldoni, & P. Gamba, "Forecasting LoRaWAN RSSI using weather parameters: A comparative study of ARIMA, artificial intelligence and hybrid approaches," *Computer Networks*, vol. 243, 110258, 2024. https://doi.org/10.1016/j.comnet.2024.110258.

[20] O. Soprun, M. Bublyk, Yu. Matseliukh, V. Andrunyk, L. Chyrun, I. Dyyak, A. Yakovlev, M. Emmerich, O. Osolinsky, A. Sachenko, "Forecasting temperatures of a synchronous motor with permanent magnets using machine learning," *Proceedings of the 2nd International*

Workshop on Modern Machine Learning Technologies and Data Science (MoMLeT+DS 2020), Volume I: Main Conference Lviv-Shatsk, Ukraine, June 2-3, 2020, pp. 95-120. https://ceur-ws.org/Vol-2631/paper8.pdf.

[21] H. Jdi, & N. Falih, "Comparison of time series temperature prediction with auto-regressive integrated moving average and recurrent neural network," *International Journal of Power Electronics and Drive Systems/International Journal of Electrical and Computer Engineering*, vol. 14, no. 2, 1770, 2024. https://doi.org/10.11591/ijece.v14i2.pp1770-1778

[22] O. Bezsonov, et al., "Using a deep learning neural network to predict flight path," *Radioelectronic and Computer Systems*, vol. 2025, no. 1, pp. 71-84, 2025. https://doi.org/10.32620/reks.2025.1.05.

[23] X. Zhang, H. Xiang, X. Xiong, Y. Wang, & Z. Chen, "Benchmarking core temperature forecasting for lithium-ion battery using typical recurrent neural networks," *Applied Thermal Engineering*, vol. 248, 123257, 2024. https://doi.org/10.1016/j.applthermaleng.2024.123257.

[24] W. Shah, J. Chen, I. Ullah, M. H. Shah, & I. Ullah, "Application of RNN-LSTM in predicting drought patterns in Pakistan: A pathway to sustainable water resource management," *Water*, vol. 16, issue 11, 1492, 2024. https://doi.org/10.3390/w16111492.

[25] O. Tolstoluzka, D. Telezhenko, "Development and training of LSTM models for control of virtual distributed systems using TensorFlow and Keras," *Radioelectronic and Computer Systems*, vol. 2024, no. 3, pp. 27-37, 2024. https://doi.org/10.32620/reks.2024.3.02.

[26] O. A. Alawi, H. M. Kamar, R. Z. Homod, & Z. M. Yaseen, "Deep learning and tree-based models for earth skin temperature forecasting in Malaysian environments," *Applied Soft Computing*, vol. 155, 111411, 2024. https://doi.org/10.1016/j.asoc.2024.111411.

[27] V. Farhangmehr, H. Imanian, A. Mohammadian, J. H. Cobo, H. Shirkhani, & P. Payeur, "A spatiotemporal CNN-LSTM deep learning model for predicting soil temperature in diverse large-scale regional climates," *The Science of the Total Environment*, vol. 968, 178901, 2025. https://doi.org/10.1016/j.scitotenv.2025.178901.

[28] M. King, S. I. Woo, & C. Yune, "Utilizing a CNN-RNN machine learning approach for forecasting time-series outlet fluid temperature monitoring by long-term operation of BHEs system," *Geothermics*, vol. 122, 103082, 2024. https://doi.org/10.1016/j.geothermics.2024.103082.

[29] S. Bamati, H. Chaoui and H. Gualous, "Enhancing battery thermal management with virtual temperature sensor using hybrid CNN-LSTM," *IEEE Transactions on Transportation Electrification*, vol. 10, no. 4, pp. 10272-10287, 2024. https://doi.org/10.1109/TTE.2024.3376515.

[30] J. Shen, W. Wu, & Q. Xu, "Accurate prediction of temperature indicators in Eastern China using a multi-scale CNN-LSTM-Attention model," *arXiv* (Cornell University), 2024. https://doi.org/10.48550/arxiv.2412.07997.

[31] I. Uluocak, M. Bilgili, "Daily air temperature forecasting using LSTM-CNN and GRU-CNN models," *Acta Geophys*., vol. 72, pp. 2107–2126, 2024. https://doi.org/10.1007/s11600-023-01241-y.

[32] Y. Zahidi, Y. Al-Amrani, Y. El Younoussi, "Deep learning CNN–LSTM hybrid approach for arabic sentiment analysis using word embedding models," *International Journal of Modern Education and Computer Science (IJMECS)*, vol. 17, no. 1, pp. 72-90, 2025. https://doi.org/10.5815/ijmecs.2025.01.06.

[33] J. Y. Ahn, Y. Kim, H. Park, S. H. Park, & H. K. Suh, "Evaluating time-series prediction of temperature, relative humidity, and CO_2 in the greenhouse with transformer-based and RNN-based models," *Agronomy*, vol. 14, issue 3, 417, 2024. https://doi.org/10.3390/agronomy14030417.

[34] Y. Fu, J. Song, J. Guo, Y. Fu, & Y. Cai, "Prediction and analysis of sea surface temperature based on LSTM-transformer model," *Regional Studies in Marine Science*, vol. 78, 103726, 2024. https://doi.org/10.1016/j.rsma.2024.103726.

[35] S. O. Abter, S. M. Jameel, H. M. Majeed, & A. H. Sabry, "Intelligent forecasting temperature measurements of solar PV cells using modified recurrent neural network," *EUREKA Physics and Engineering*, vol. 3, pp. 169–177, 2024. https://doi.org/10.21303/2461-4262.2024.003354.

[36] Humid Continental (Group D), Physical Geography. (n.d.). [Online]. Available at: https://courses.lumenlearning.com/suny-geophysical/chapter/humid-continental-group-d/.

[37] Kaggle. Globallandtemperature, 2018. [Online]. Available at: https://www.kaggle.com/datasets/sambapython/globallandtemperature. (accessed on 11 February 2025).

[38] *Global Historical Weather and Climate Data*, *Weather and Climate*, 2025. [Online]. Available at: https://weatherandclimate.com/. (accessed on 15 February 2025).

[39] M. Waqas, & U. W. Humphries, "A critical review of RNN and LSTM variants in hydrological time series predictions," *MethodsX*, vol. 13, 102946, 2024. https://doi.org/10.1016/j.mex.2024.102946.

[40] N. Yehia, & N. Yehia, "Understanding long short-term memory (LSTM) networks," *Machine Learning Archive*, 2024. [Online]. Available at: https://mlarchive.com/deep-learning/understanding-long-short-term-memory-networks/.

[41] GeeksforGeeks, What is LSTM long short term memory? 2024. [Online]. Available at: https://www.geeksforgeeks.org/deep-learning-introduction-to-long-short-term-memory/ (accessed on 10 January 2025).

***TETIANA HOVORUSHCHENKO** DrSc (Engineering), Dean of the Faculty of Information Technologies, Professor of Computer Engineering & Information Systems Department, Khmelnytskyi National University, Ukraine. Research interests: Software quality assessment; Intelligent agents based on the ontological approach; Intelligent information systems and technologies.*

***OLGA PAVLOVA** PhD, Associate professor of Computer Engineering & Information Systems Department, Khmelnytskyi National University, Ukraine. Research interests: Agent-oriented information technology for assessing the initial stages of the software life cycle based on the ontological approach.*

***VITALII ALEKSEIKO**, PhD Student majoring in Information Systems and Technologies, Assistant Lecturer of Computer Engineering & Information Systems Department, Khmelnytskyi National University, Ukraine. Research interests: Using AI technologies in applied tasks, Machine Learning, Responsible use and ethical aspects of artificial intelligence.*

***ANDRII KUZMIN** Master student majoring in Computer Engineering, Khmelnytskyi National University, Ukraine. Research interests: Artificial Intelligence, Computer Vision.*

***ELENA ZAITSEVA** Associate Professor of Department of Informatics, Faculty of Management Science and Informatics, University of Žilina, Slovakia. Research interests: Multiple-Valued Logic, Artificial Intelligence, Reliability Analysis for Multi-State System, Application of Reliability Analysis Methods in Medicine.*